Ecotoxicology and Environmental Safety 169 (2019) 583–589

Contents lists available at ScienceDirect

Ecotoxicology and Environmental Safety

journal homepage: www.elsevier.com/locate/ecoenv

Structural characteristics of cake layer in membrane bioreactor with chromate exposure

Lijie Zhou[a,*], Biao Ye[b], Siqing Xia[b,*]

[a] College of Chemistry and Environmental Engineering, Shenzhen University, Shenzhen 518060, PR China
[b] State Key Laboratory of Pollution Control and Resource Reuse, Shanghai Institute of Pollution Control and Ecological Security, College of Environmental Science and Engineering, Tongji University, 1239 Siping Road, Shanghai 200092, PR China

ARTICLE INFO

Keywords:
Cake layer
Chromate exposure
Membrane bioreactor
Structural characteristics

ABSTRACT

Chromate (CrO_4^{2-}) exposure, especially high concentration (mg/L), still probably occurs in the industrial and mining area due to industrial accidents or even illegal discharge, though CrO_4^{2-} has been restricted to be discharged into wastewater treatment system (WWTS). Therefore, this study was applied to better understand the structural characteristics of cake layer in membrane bioreactor (MBR), which is one of best alternative for WWTS of industrial or mining area, with CrO_4^{2-} exposure. Three submerged MBRs with CrO_4^{2-} exposure (10 mg/L was normal high concentration CrO_4^{2-}; 50 mg/L as extreme level for better identification; 0 mg/L as control condition) were applied in this study. Results showed that CrO_4^{2-} exposure caused an obvious variation of cake layer structure. Because of organic component variation, cake layer structure with CrO_4^{2-} exposure was re-constructed into loose and porous with biomicromolecules, and resulted in the rapid cake layer thickness increase, finally leading to severe membrane biofouling. Additionally, CrO_4^{2-} distributed evenly along the cross-sectional cake layer. CrO_4^{2-} only induced the inorganic structure variations of cake layer, but without any obvious effects on the other inorganic elements structure. CrO_4^{2-} exposure induced the bacterial community structure variation and led to tolerated-CrO_4^{2-} microorganisms as the majority in cake layer community, but had no obvious effects on the population diversity.

1. Introduction

Membrane bioreactor (MBR), coupling biological treatment and membrane separation, has been regarded as one of most effective methods for wastewater treatment, especially in the industrial and mining area normally locating at countryside or small town with low population (Gao et al., 2011; Mutamim et al., 2013; Xiong et al., 2016; Zhou et al., 2014a). Over recent decades, obvious progress has been achieved in the research and application of MBR due to its advantages (i.e., high effluent quality, small footprint, low sludge production) over conventional activated sludge (Hu et al., 2016). Derivative MBRs, such as ultrafiltration MBR (Xia et al., 2010), nonwoven MBR (Wang et al., 2015), osmotic MBR (Aftab et al., 2017), etc., have also been carried out, studied and applied, but MBR with microfiltration is still the mainstream technology for pilot or full scale application (Gurung et al., 2017). However, membrane biofouling and its cake layer are still the obstacle for MBR operation, which directly increases the operational cost and further limits the widespread application of MBR (Gao et al., 2011; Zhu et al., 2016).

Membrane biofouling is a complex interaction process between membrane and mixed liquid components, and its cake layer involves bacteria, suspended solids, extracellular substances (ES), biomicromolecules, inorganic substances, biomacromolecules, colloids, etc. (Hu et al., 2016). Based on previous studies (Gao et al., 2013, 2012; Zhu et al., 2016), organic components in cake layer, especially ES, are widely accepted as the primary biofouling-causing substances and the major component within the cake layer. Moreover, recent studies (Gao et al., 2011; Hu et al., 2016; Miao et al., 2017; Zhu et al., 2016) are focused on the structural characteristics of cake layer during MBR operation for better understanding of cake layer, to further carry out promising membrane biofouling mitigation methods. Additionally, inorganic components in cake layer, especially metal cations (Mg^{2+}, Ca^{2+}, Al^{3+}, Fe^{3+}, etc.), were reported to accumulate into cake layer, and cause an obvious structural characteristics of cake layer (Arabi and Nakhla, 2009; Chen et al., 2011; Miao et al., 2017; Zhou et al., 2014b). Zhou et al. (2014b) reported that Ca^{2+} had no effects on cake layer thickness but inhibited the deposition of Mg^{2+}, Al^{3+}, Fe^{3+}, etc., onto the membrane surface, finally leading to the porous structure of cake

* Corresponding authors.
E-mail addresses: pakerzhou@szu.edu.cn (L. Zhou), siqingxia@tongji.edu.cn (S. Xia).

https://doi.org/10.1016/j.ecoenv.2018.11.056
Received 5 September 2018; Received in revised form 1 November 2018; Accepted 14 November 2018

layer. Miao et al. (2017) showed that Al^{3+} and Fe^{3+} presented the opposite effects on the structural characteristics of cake layer, especially the microbial community of cake layer. Furthermore, inorganic components, especially heavy metal, in the environment and their flow in the wastewater treatment system also the heat topic in the environmental science and engineering area (Hooda, 2010; Johannesson and Tang, 2009; Nicholson et al., 2003). However, although effects of metal cations on cake layer structure have been studied, the knowledge about effects of metal anions, especially chromate (CrO_4^{2-}), on cake layer is limited.

CrO_4^{2-}, known as the typical metal anion, is one of the most widely applied heavy metals with commercial and industrial importance, and significant amounts of CrO_4^{2-} are released into wastewater, especially in the industrial and mining area (Vaiopoulou and Gikas, 2012). CrO_4^{2-} is also one of the most toxic metals, which can lead to carcinoma, chromosomal mutations/aberrations, DNA damage, etc. CrO_4^{2-} easily discharges into groundwater or wastewater due to its high solubility (Gorny et al., 2016). Currently, CrO_4^{2-}, widely remaining in groundwater, wastewater, soil and sediments, has become one of the most hazardous materials for the environment, especially in the industrial and mining area (Gu et al., 2017; Hausladen and Fendorf, 2017; Liu et al., 2017). From 1952–1966, Pacific Gas and Electric Company (PG& E) dumped roughly 370 million gallons of Cr-contained wastewater into the environment around the small town of Hinkley (California, USA). In 2011, over 5000 t CrO_4^{2-}-contained waste was illegally dropped into the environment around the countryside of Qujing (Yunnan, China), causing severe CrO_4^{2-} pollution with over 100 mgCr(VI)/L in aquatic environment. During January to June of 2017, an electroplate workshop in the village of Kunshan (Suzhou, China) illicitly discharged untreated wastewater with approximately 240 mgCr(VI)/L into the environment. It could be hypothesized that CrO_4^{2-} exposure, especially high concentration of over 10 mgCr(VI)/L, would happen to local wastewater treatment system in the industrial and mining area due to polluted water utilization and rainfall. Additionally, as one of best alternative for wastewater treatment system of industrial and mining area, MBR normally locates in the countryside or small town with low population. Consequently, CrO_4^{2-} exposure, especially high concentration of over 10 mgCr(VI)/L, would be a toxicity shock for MBR operation. Zhao et al. (2009) reported that CrO_4^{2-} could change the morphology of activated sludge, further inhibiting membrane filtration and leading to severe membrane biofouling. Zhou et al. (2014a) also found that CrO_4^{2-} exposure led to severe irreversible membrane pore blocking and markedly shortened the service life of the membrane module. However, the structural characteristics of cake layer with CrO_4^{2-} exposure is still unclear, especially insights into the inner structure of cake layer.

This study aims to develop an improved fundamental understanding of the structural characteristics of cake layer in MBR with CrO_4^{2-} exposure, especially high concentration. Therefore, high concentrations of 10 and 50 mg/L CrO_4^{2-} were applied in this study. 10 mg/L CrO_4^{2-} was normally considered as the high concentration, and 50 mg/L CrO_4^{2-} (this level would not be found in real world) was mainly applied for better understanding the structural characteristics of cake layer in MBR with CrO_4^{2-} exposure. Cake layer structure was identified with ES analysis, SEM-EDX (scanning electron microscopy-energy dispersive X-ray analyzer), microscope, bacterial community, viscosity, etc. in this study. Batch experiment for CrO_4^{2-} distribution was also carried out for tracing CrO_4^{2-} in the cake layer.

2. Materials and methods

2.1. Set-up and operation

Three parallel submerged MBRs were operated with CrO_4^{2-} exposure (K_2CrO_4 as the CrO_4^{2-} source) at 0 mg/L, 10 Cr mg/L and 50 Cr mg/L, respectively. A polyvinylidene fluoride (PVDF) hollow fiber membrane module (0.4 μm nominal pore size; 10 dm^2 effective filtration area; Li-tree Company, Suzhou, China) was mounted at the reactor bottom. MBRs were maintained at 30 days SRT (solid retention time) and 8 h HRT (hydraulic retention time). The flux was controlled with the intermittent filtration mode (10 min suction followed by 2 min relaxation), and 0.6 m^3/h aeration was provided continuously through an axial perforated tube below the membrane modules.

Inoculating biomass was drawn from the return activated sludge stream in the Quyang wastewater treatment plant (Shanghai, China). The newly inoculated MBRs were initially operated with gradual CrO_4^{2-} increase to achieve stable pollutants removal (COD_{Cr}, NH_4^+-N, etc.) and steady CrO_4^{2-} concentration in sludge for the acclimatization of activated sludge. The membrane module was then replaced with a new unit and MBRs were operated over 80 days for the experiments. When the transmembrane pressure (TMP) reached 40 kPa, the membrane module was cleaned for physical (washing with tap water) and chemical methods (1% NaOCl and 10% citric acid immersion for 6 h, respectively) to recover the membrane permeability. Influent characteristics are shown in SI (Supporting Information).

2.2. Extraction and measurement of ES in cake layer

ES in cake layer was extracted according to the modified thermal extraction method (Zhou et al., 2014c). Cake layer was scraped from membrane surface and dissolved in 10 mL 0.9% NaCl. The solution was treated by ultrasound (DS510DT, 40 kHz, 300 W, Shangchao, China) for 8 min and then shaken at 150 rpm for 10 min. Then the solution was heated at 80 °C for 30 min and centrifuged at 12000 g (MILTIFUGE X1R, Thermo Electron Corporation, USA) for 20 min. The supernatant was regarded as ES of cake layer. Polysaccharide and protein are considered as the major components that play significant roles in ES of cake layer. Polysaccharide and protein were measured with the phenol-sulfuric acid method and Branford method, respectively. ES of activated sludge was extracted with the same modified thermal method.

2.3. SEM-EDX and microscope measurement

For each cake layer sample, a piece of membrane fiber was cut from the middle section of the membrane module after liquid-nitrogen freezing pretreatment. 3 replicate samples in each condition were measured for SEM-EDX analysis. Cake layer was characterized with SEM (XL30, Philips, Netherlands) coupled with an EDX (Oxford Isis, UK). In addition, the thickness of cake layer was also detected with SEM-EDX measurement.

2.4. 16s rRNA gene-cloning and phylogenetic analysis

Tap water was applied as the synthetic wastewater source in this study, and the amount of total bacteria in tap water should be less than 100 CFU/mL according to Standards for Drinking Water Quality of China (GB 5749-2006). It means that the synthetic wastewater in this study should contain much fewer bacteria than that in the MBR system. Moreover, the bacterial community of activated sludge was reported to play an important role in cake layer formation (Takada et al., 2018). Therefore, this study was focused on the bacterial community of activated sludge, and ignored the bacteria in the synthetic wastewater. Cloning library was applied to identify the bacterial community of activated sludge. Genomic DNA of the sample was extracted with a FastDNA Spin Kit (MP Biomedicals, LLC, France). The procedure of cloning library was completed according to papers (Xia et al., 2012, 2010). 100 positive clones were selected for sequencing for each sample, and all the sequences were compared to the known sequences for phylogenetic analysis. Operational taxonomic units (OTUs) were defined as groups in which the sequence similarity was more than 97%. Phylogenetic trees were constructed by neighbor-joining method with the Clustal X software package. 16 s rRNA gene sequences from this study have been

submitted to National Center for Biotechnology Information (NCBI) public databases (GenBank) under accession numbers KT182476 to KT182554. Phylogenetic tree was analyzed with software Megan (version 5.8.6).

2.5. Analyses of other parameters

Chemical oxygen demand (COD_{Cr}), ammonia (NH_4^+-N), and mixed liquor suspended solids (MLSS) were performed according to the standard methods (APHA, 1998). Dissolved oxygen (DO) and pH were measured with a DO-and-pH meter (HQ4d, HACH, USA). Molecular weight (MW) distribution of ES in cake layer was determined with a gel filtration chromatography (GFC; with a TSK G4000SW type gel column (TOSOH Corporation, Japan) and a liquid chromatography spectrometer (LC-10ATVP, SHIMADZU, Japan)) analyzer. Viscosity of cake layer and activated sludge was measured with DV-C viscometer (Brookfield, USA).

CrO_4^{2-} was analyzed with the reaction with 1,5-diphenylcarbazide and measurement on UV–VIS spectrophotometer (4802 UV/VIS, UNICO, USA) at 540 nm. Concentrations of inorganic elements in the influent, effluent, activated sludge and cake layer were analyzed with an inductively coupled plasma-optical emission spectrometer (ICP-OES, Optima 2100 DV, Perkin Elmer, USA) according to Standard Methods (China-NEPA, 2002). Other items, such as membrane resistance, FTIR (Fourier transform infrared) spectra, dehydrogenase, etc., were detailed in SI.

3. Results and discussion

3.1. Reactor performance and biofouling behavior

During 80 days operation, MBRs exhibited steady-state performance with CrO_4^{2-} exposure. As Table 1 shows, although CrO_4^{2-} exposure had no obvious effects on COD_{Cr} removal, it significantly inhibited NH_4^+-N removal (dropped from 95 ± 3% to 38 ± 5%). Additionally, CrO_4^{2-} exposure led to the obvious decrease of MLSS from 3.43 to 2.85 g/L, predicting the toxicity of CrO_4^{2-} exposure to biomass. Fig. 1 further shows the CrO_4^{2-} reduction performance of MBR-10 ppm and MBR-50 ppm. MBR-10 ppm and MBR-50 ppm had slight removal of total CrO_4^{2-} at approximate 3% and 1%, respectively. In the effluent of both MBR-10 ppm and MBR-50 ppm, most of Cr was in the form of CrO_4^{2-}, meaning that less Cr was transferred from CrO_4^{2-} to Cr^{3+} through submerged MBR system. Hexavalent chromium is less stable than trivalent form, and it was reported that CrO_4^{2-} could be reduced and transformed into Cr^{3+} with anaerobic biological treatment, especially in the presence of organic matter (Gu and Chen, 2003; Thatoi et al., 2014; Vatsouria et al., 2005). However, in the submerged MBR system, strong air bubbling supplied high oxygen to reactor and could obviously inhibit the CrO_4^{2-} to Cr^{3+} reduction process of activated sludge (Vaiopoulou and Gikas, 2012; Xia et al., 2015). Additionally, 10 and 50 mg/L of CrO_4^{2-} were too high for biological removal and thus both MBRs showed the low CrO_4^{2-} reduction performance in this study (Thatoi et al., 2014; Vaiopoulou and Gikas, 2012). Consequently, MBR-

Table 1
Operating conditions of three MBRs.

Parameter	MBR-Blank	MBR-10 ppm	MBR-50 ppm
Influent CrO_4^{2-} concentration (mg Cr/L)	–	10	50
Dissolved oxygen (mg/L)	6.0	6.0	6.0
pH	7.0	7.0	7.0
MLSS (g/L)[a]	3.43 ± 0.54	2.84 ± 0.31	2.85 ± 0.14
COD_{Cr} removal efficiency (%)[a]	89 ± 5	88 ± 3	85 ± 2
NH_4^+-N removal efficiency (%)[a]	95 ± 3	85 ± 8	38 ± 5

[a] n = 30.

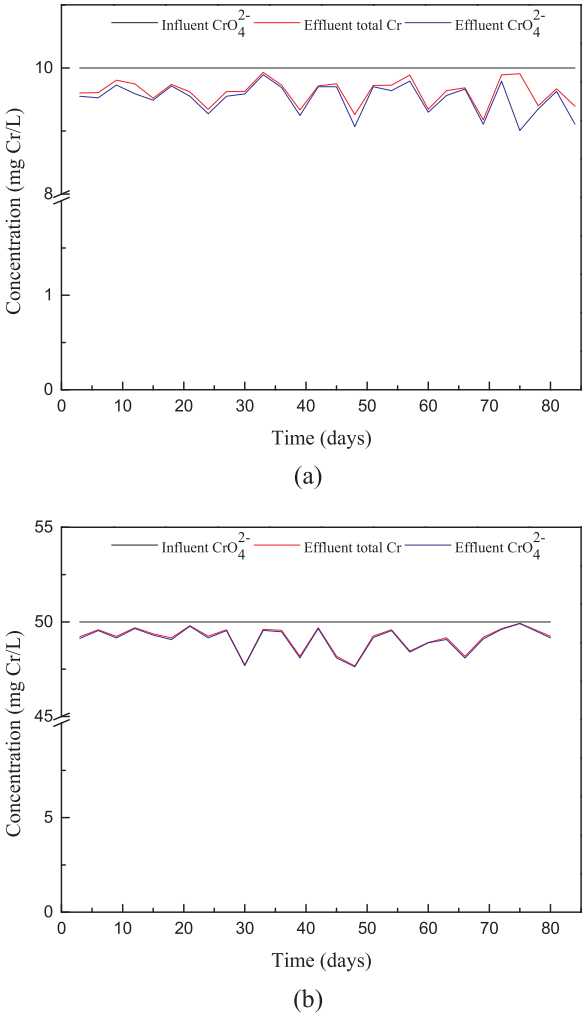

Fig. 1. Reduction of CrO_4^{2-} in (a) MBR-10 ppm and (b) MBR-50 ppm. (All Cr in the influent was in the form of CrO_4^{2-}, meaning that total Cr concentration was equal to CrO_4^{2-} concentration in the influent.).

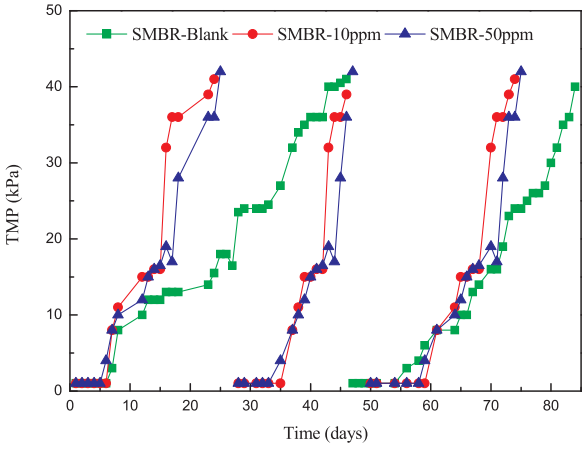

Fig. 2. TMP variation with CrO_4^{2-} exposure.

10 ppm and MBR-50 ppm showed the low performance for CrO_4^{2-} reduction, and few CrO_4^{2-} could be transformed into Cr^{3+} due to strong air supplement.

Given that TMP is an important index for evaluating membrane performance, its development rate directly reflects the extent of membrane biofouling. Biofouling can be classified into slight TMP increase

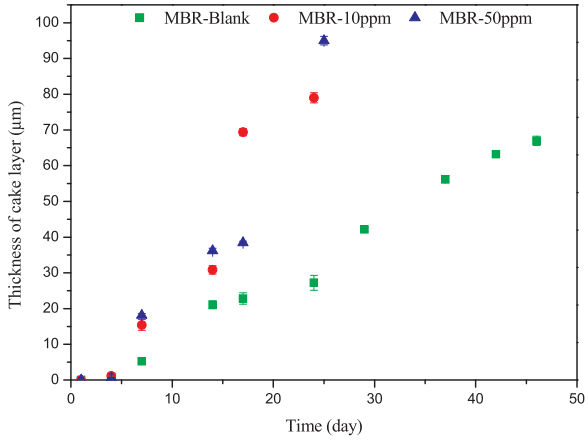

Fig. 3. Thickness variations of cake layer with CrO_4^{2-} exposure (n = 3).

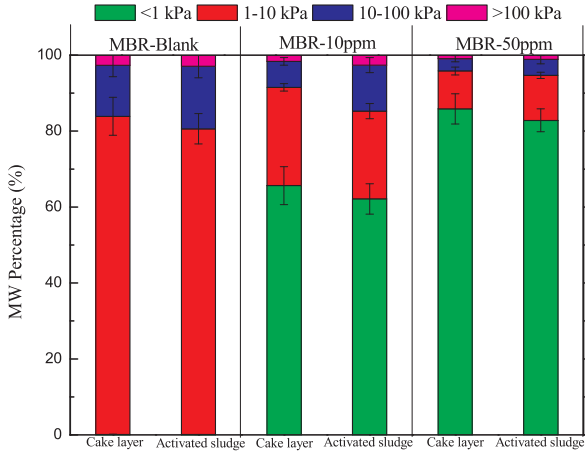

Fig. 4. MW distribution of ES in cake layer and activated sludge with CrO_4^{2-} exposure.

or rapid one, and rapid one mainly presents the cake layer formation (Zhou et al., 2014c). The development rate of rapid TMP increase was 1.3 kPa/day in MBR-Blank, and the rate with CrO_4^{2-} exposure increased to approximately 2.0 kPa/day (Fig. 2), indicating that CrO_4^{2-} exposure aggravated the formation of cake layer. In addition, the resistances of cake layer is also measured in this study. Total resistance of membrane (R_t) in MBR-10 ppm contained $(0.10 \pm 0.01)\times 10^{12}$ m^{-1} R_p (pore blocking resistance), $(8.75 \pm 0.8)\times 10^{12}$ m^{-1} R_c (fouling layer resistance), $(0.14 \pm 0.01)\times 10^{12}$ m^{-1} R_m (resistance of the clean membrane). R_t in MBR-50 ppm contained $(0.07 \pm 0.02)\times 10^{12}$ m^{-1} R_p, $(8.96 \pm 0.05)\times 10^{12}$ m^{-1} R_c, $(0.14 \pm 0.01)\times 10^{12}$ m^{-1} R_m. But, R_t in MBR-Blank contained $(0.08 \pm 0.01)\times 10^{12}$ m^{-1} R_p, $(3.35 \pm 0.04)\times 10^{12}$ m^{-1} R_c, $(0.14 \pm 0.01)\times 10^{12}$ m^{-1} R_m. Increasing total resistance indicated that CrO_4^{2-} exposure led to the severe membrane biofouling. R_c in MBR-10 ppm and MBR-50 ppm are also over twice of that in MBR-Blank, predicting that CrO_4^{2-} exposure aggravated the biofouling behavior mainly due to the structural characteristics variations of cake layer.

3.2. Physicochemical characteristics of cake layer with CrO_4^{2-} exposure

Physicochemical characteristics of cake layer is first identified with SEM. Fig. S1 presents that CrO_4^{2-} exposure varied cake layer surface from dense to porous. The thickness variations of cake layer with CrO_4^{2-} exposure are shown in Fig. 3. The final thickness of cake layer are 67, 79 and 95 μm, respectively, in MBR-Blank, MBR-10 ppm and MBR-50 ppm. CrO_4^{2-} exposure obviously increased cake layer thickness. In addition, the cake layer thickness growth rate increased from 1.7 to 4.1 μm/day, indicating that CrO_4^{2-} exposure effectively aggravated the cake layer formation. Therefore, even though CrO_4^{2-} re-structured cake layer into loose and porous form, it still promoted the cake layer formation and increased the cake layer thickness.

Fig. 4 also shows that CrO_4^{2-} exposure reduced the MW of ES in cake layer, and < 1 kPa components contributed over 60% of cake layer with CrO_4^{2-} exposure, meaning that CrO_4^{2-} induced the biomacromolecule decrease of ES in cake layer. In addition, Table 2 shows the viscosities of cake layer and the activated sludge were reduced with CrO_4^{2-} exposure, indicating the bonding capacity decrease of organic components. Moreover, as previous studies (Johannesson and Tang, 2009; Nicholson et al., 2003) reported, flow is also very important in the water system. Meng et al. (2009) reviewed that proteins and polysaccharides could be deposited onto the membranes more readily for cake layer formation due to the permeate flow. Thus, low viscosity could lead to the permeate flow enhancement, and further promote the cake layer formation. In addition, CrO_4^{2-} exposure caused biomacromolecule decrease of ES, and fast permeate flow would contribute to the formation of loose and porous cake layer at early stage (Choi et al., 2005; Yang et al., 2016). Thus, results of MW and viscosity partly explained the loose and porous structure of cake layer with CrO_4^{2-} exposure.

However, Table 2 shows that CrO_4^{2-} exposure significantly increased polysaccharide and protein of ES in both cake layer and activated sludge. Polysaccharide and protein in cake layer were slightly higher than those in activated sludge, which is because of the suction pressure to cake layer during membrane operation. Furthermore, the protein secretion in the cake layer (also in activated sludge) was due to the toxicity of CrO_4^{2-} exposure and the respect of bacterial immune system (Xia et al., 2015). Dehydrogenase of activated sludge in MBR-10 ppm and MBR-50 ppm were only 82 ± 4% and 76 ± 6%, respectively, of that in MBR-Blank, which further proves the toxicity of CrO_4^{2-} exposure. FTIR (Fig. S2) was also carried out to identify the physicochemical characteristics of cake layer. The IR peak at 1255 cm^{-1} was presented due to the CrO_4^{2-} exposure, indicating the combination between $(SOH)_2$ and CrO_4^{2-} (Xia et al., 2015). Cake layer with CrO_4^{2-} exposure also had the complex IR peaks ranging < 1000 cm^{-1}, which is the range for the connection between metals and functional groups. It indicated that cake layer contained CrO_4^{2-} in its bonded form with its organic components.

In all, CrO_4^{2-} exposure increased the polysaccharide and protein of ES in cake layer, but also re-constructed the functional groups

Table 2
Polysaccharide (mg/g dry cake layer or activated sludge), protein (mg/g dry cake layer or activated sludge) in ES and viscosity (mPa/s) of cake layer and activated sludge with CrO_4^{2-} exposure. (n = 6).

	MBR-Blank		MBR-10 ppm		MBR-50 ppm	
	Bio.	Act.	Bio.	Act.	Bio.	Act.
Pol.[a]	38 ± 2	34 ± 5	58 ± 4	43 ± 3	67 ± 5	60 ± 3
Pro.[a]	34 ± 7	30 ± 3	73 ± 3	58 ± 5	87 ± 7	73 ± 8
Vis.[a]	13.4 ± 1.4	9.7 ± 1.3	6.3 ± 0.5	4.6 ± 0.7	5.2 ± 1.0	3.1 ± 0.4

[a] Pol.: polysaccharide in ES; Pro.: protein in ES; Vis.: viscosity; Bio.: cake layer; Act.: activated sludge.

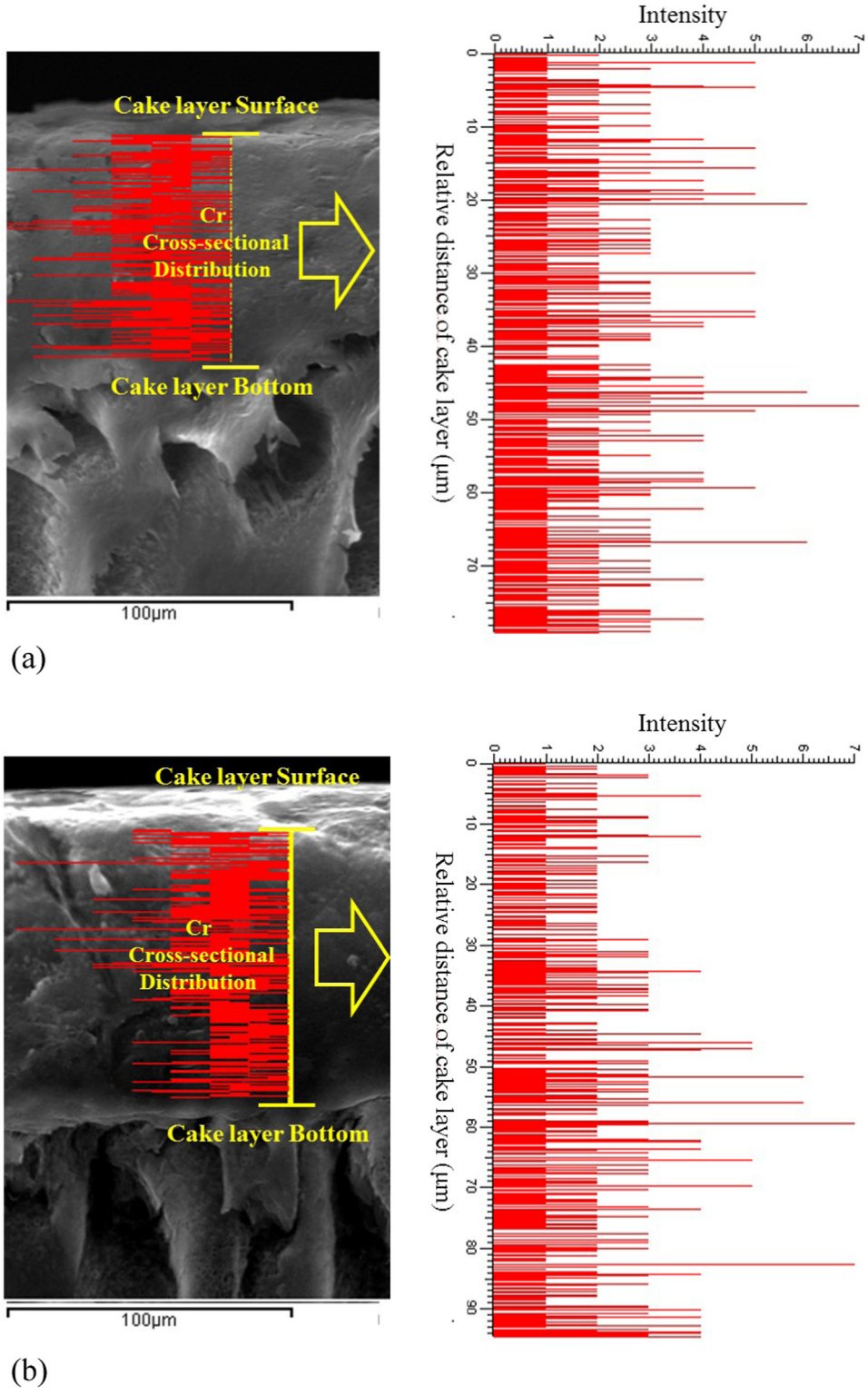

Fig. 5. Cr cross-sectional distribution of cake layer in (a) MBR-10 ppm and (b) MBR-50 ppm.

combination, decreased MW of ES, reduced the viscosity of cake layer, before finally reducing organic components bonding. Therefore, cake layer constructed biomicromolecules under CrO_4^{2-} exposure, but restructured into loose and porous. The severe membrane biofouling was relied on the rapid thickness increase of cake layer with high organic components (polysaccharide, protein, etc.).

3.3. Cr distribution in cake layer with CrO_4^{2-} exposure

Inorganic structure, especially its distribution, works as the significant role in membrane biofouling and cake layer. Table 1 shows that most of the CrO_4^{2-} passed through the membrane, predicting that membrane could not intercept CrO_4^{2-} in the reactor. In addition, based on Fig. 1 and previous literatures (Vaiopoulou and Gikas, 2012; Xia et al., 2015), few CrO_4^{2-} were reduced into Cr^{3+} under condition of

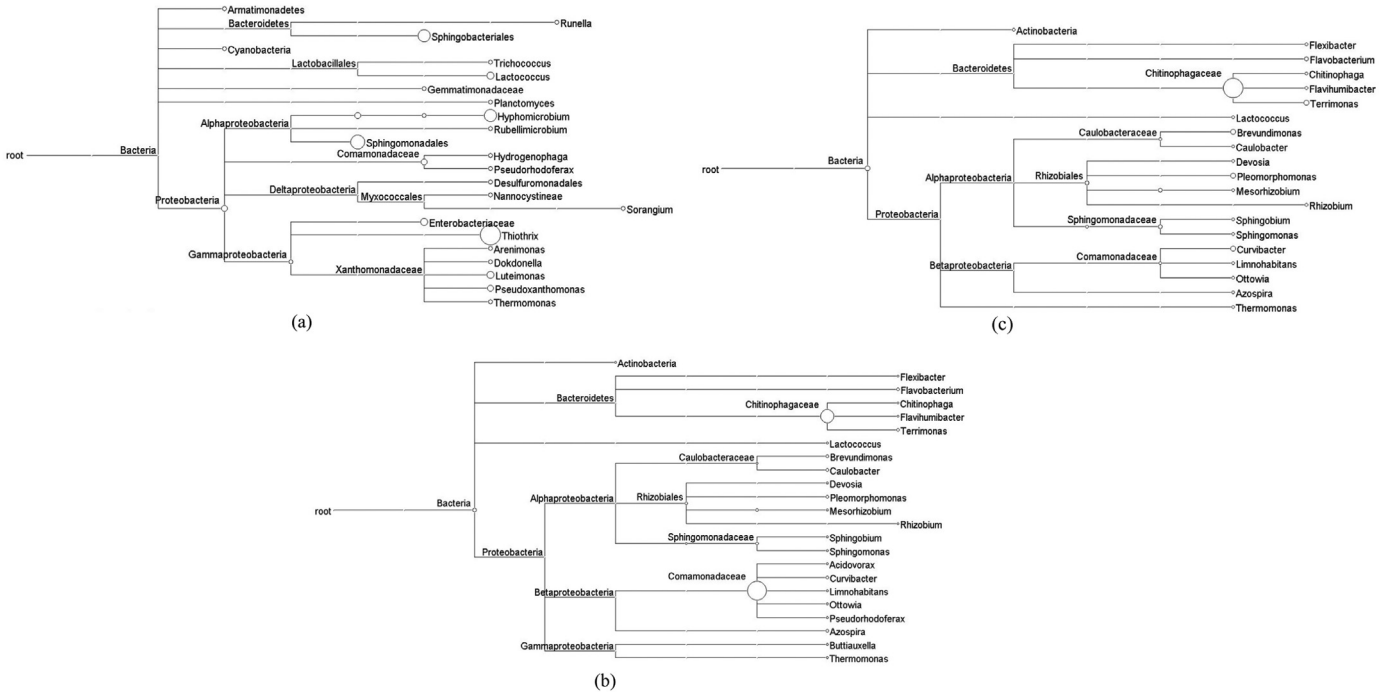

Fig. 6. Phylogenetic tree of cake layer in (a) MBR-Blank, (b) MBR-10 ppm and (c) MBR-50 ppm.

high DO, and thus the reduction of CrO_4^{2-} into Cr^{3+} could be ignored in this study. Therefore, Fig. 5 shows Cr cross-sectional distribution of cake layer in MBR-10 ppm and MBR-50 ppm, which mainly predicted the CrO_4^{2-} distribution in the cake layer. CrO_4^{2-} distributed evenly through the cross-sectional cake layer (Fig. 5), and the cake layer contained approximately 1.25 mg CrO_4^{2-}/g cake layer during cake layer growth (Fig. S3), indicating that CrO_4^{2-} contributed to the cake layer structure under a stable biofouling behavior. The similar CrO_4^{2-} distribution with both 10 and 50 mg/L CrO_4^{2-} exposure and results of CrO_4^{2-} in the effluent indicated that CrO_4^{2-} only partly accumulated in the cake layer, and most of the CrO_4^{2-} flowed through the membrane, which should be due to its ion form (Fu and Wang, 2011). Additionally, batch experiments for CrO_4^{2-} distribution (SI) were also applied for better understanding the CrO_4^{2-} behavior in the cake layer during membrane filtration. According to CrO_4^{2-} removal and previous reviews (Pradhan et al., 2016; Vaiopoulou and Gikas, 2012), CrO_4^{2-} in the cake layer was classified into free ions of CrO_4^{2-} (in the liquid phase of cake layer), CrO_4^{2-} in accumulation (in the solid phase of cake layer) and CrO_4^{2-} with suction pressure (in the liquid phase through membrane module). In batch experiment for CrO_4^{2-} distribution in cake layer, CrO_4^{2-} with suction pressure (92%) dominated the CrO_4^{2-} distribution in cake layer, and only a few Cr were in the form of free CrO_4^{2-} (5%) and CrO_4^{2-} in accumulation (3%), indicating that cake layer was tolerated with treble CrO_4^{2-} exposure (Fig. S4) and most of the CrO_4^{2-} outflowed through cake layer. Therefore, only a minority of CrO_4^{2-} were involved in the cake layer structure during filtration, and most of CrO_4^{2-} was discharged into effluent through cake layer.

In addition, Al, Ca and Mg are also reported as important compounds in the inorganic structure of cake layer. As Fig. S5 to S8 shows, CrO_4^{2-} exposure had no obvious effects on the distribution of Al, Ca and Mg in the cake layer. It was because CrO_4^{2-}, even at high concentration, would not precipitate with Al, Ca and Mg. Moreover, Al^{3+}, Fe^{3+}, Ca^{2+} and Mg^{2+} would not obviously compete with CrO_4^{2-} for bonding with organic components, because of their different ion charge. Consequently, CrO_4^{2-} only led to the inorganic structure variation of cake layer, but without any effects on other inorganic elements structure.

3.4. Bacterial community structure of cake layer with CrO_4^{2-} exposure

The 16 s rDNA clone library (Fig. 6) shows that 23, 23 and 20 OTUs were obtained from cake layer of MBR-Blank, MBR-10 ppm and MBR-50 ppm, respectively, indicating that CrO_4^{2-} exposure had no obvious effect on the population diversity of cake layer bacterial community. In addition, the phylogenetic tree of cake layers (Fig. 6) shows the dominate bacteria in MBR-Blank, such as *Sphingobacterales*, *Hyphomicrobium*, *Thiothrix* (known as denitrifier (Trubitsyn et al., 2014)), etc., were reduced with CrO_4^{2-} exposure. Fig. 6(a) and (b) shows that *Chitinophagaceae*, reported in denitrifying consortia (Zhong et al., 2017), predominated rapidly with CrO_4^{2-} exposure, meaning that *Chitinophagaceae* replaced the denitrification role of *Thiothrix*. Additionally, *Rhizobiales* and *Sphingomonadaceae*, the dichromate and biofilm species (Naz et al., 2016), also increased with CrO_4^{2-} exposure and became the major bacteria in cake layer. As batch experiment for CrO_4^{2-} distribution in cake layer shows, microorganisms in cake layer were tolerated with treble CrO_4^{2-} during membrane filtration. Treble CrO_4^{2-} led to *Caulobacter*, *Pleomorphomonas*, *Mesorhizobium*, *Rhizobium*, *Sphingobium*, *Azospira*, *Flexibacter*, etc., the tolerated-CrO_4^{2-} bacteria (Kohler et al., 2012; Naz et al., 2016; Porter et al., 2017; Pradhan et al., 2016; Samaras et al., 2009), became the dominating species in the cake layer. Consequently, cake layer tolerated with treble CrO_4^{2-} exposure, induced the bacterial community structure variation, and led to tolerated-CrO_4^{2-} microorganisms as the dominant species in cake layer community, but without any obvious effects on the population diversity.

4. Conclusions

Cake layer had the obvious variation of structural characteristics with CrO_4^{2-} exposure. Due to organic components, cake layer structure with CrO_4^{2-} exposure was re-constructed into loose and porous with biomicromolecules, and resulted in the rapid cake layer thickness increase, finally leading to severe membrane biofouling. CrO_4^{2-} distributed evenly along the cross-sectional cake layer. CrO_4^{2-} only caused the inorganic structure variations of cake layer with treble CrO_4^{2-} exposure, but without any effects on other inorganic elements structure. CrO_4^{2-} exposure induced the bacterial community structure variation

and led to tolerated-CrO_4^{2-} microorganisms as the majority in cake layer community, but CrO_4^{2-} exposure had no obvious effects on the population diversity.

Acknowledgments

This study was funded by “Project 51708362 and 51678422 supported by National Natural Science Foundation of China”, “State Key Laboratory of Pollution Control and Resource Reuse Foundation (NO. PCRRF17025)”, “National Key Research and Development Program of China (2017YFC0403403)” and “Natural Science Foundation of SZU (827-000282)”.

Appendix A. Supplementary material

Supplementary data associated with this article can be found in the online version at doi:10.1016/j.ecoenv.2018.11.056.

References

Aftab, B., et al., 2017. Heavy metals removal by osmotic membrane bioreactor (OMBR) and their effect on sludge properties. Desalination 403, 117–127.
APHA, 1998. Standard Methods for the Examination of Water and Wastewater. American Pubilc Health Association, Washington, DC, USA.
Arabi, S., Nakhla, G., 2009. Impact of cation concentrations on fouling in membrane bioreactors. J. Membr. Sci. 343, 110–118.
Chen, K., et al., 2011. Impacts of sludge retention time on the performance of submerged membrane bioreactor with the addition of calcium ion. Sep. Purif. Technol. 82, 148–155.
China-NEPA, 2002. Water and Wastewater Monitoring Methods. Chinese Enviromental Science Publishing House, Beijing, China.
Choi, H., et al., 2005. Influence of cross-flow velocity on membrane performance during filtration of biological suspension. J. Membr. Sci. 248, 189–199.
Fu, F., Wang, Q., 2011. Removal of heavy metal ions from wastewaters: a review. J. Environ. Manag. 92, 407–418.
Gao, D.W., et al., 2013. Tracing biofouling to the structure of the microbial community and its metabolic products: a study of the three-stage MBR process. Water Res. 47, 6680–6690.
Gao, W.J., et al., 2011. Structure of cake layer in a submerged anaerobic membrane bioreactor. J. Membr. Sci. 374, 110–120.
Gao, W.J., et al., 2012. Influence of temperature and temperature shock on sludge properties, cake layer structure, and membrane fouling in a submerged anaerobic membrane bioreactor. J. Membr. Sci. 421, 131–144.
Gorny, J., et al., 2016. Chromium behavior in aquatic environments: a review. Environ. Rev. 24, 503–516.
Gu, B.H., Chen, J., 2003. Enhanced microbial reduction of Cr(VI) and U(VI) by different natural organic matter fractions. Geochim. Et. Cosmochim. Acta 67, 3575–3582.
Gu, X.Y., et al., 2017. A simple model to predict chromate partitioning in selected soils from China. J. Hazard. Mater. 322, 421–429.
Gurung, K., et al., 2017. Assessing membrane fouling and the performance of pilot-scale membrane bioreactor (MBR) to treat real municipal wastewater during winter season in Nordic regions. Sci. Total Environ. 579, 1289–1297.
Hausladen, D.M., Fendorf, S., 2017. Hexavalent chromium generation within naturally structured soils and sediments. Environ. Sci. Technol. 51, 2058–2067.
Hooda, P.S., 2010. Assessing Bioavailability of Soil Trace Elements. John Wiley & Sons, Ltd.
Hu, Y.S., et al., 2016. New insight into fouling behavior and foulants accumulation property of cake sludge in a full-scale membrane bioreactor. J. Membr. Sci. 510, 10–17.
Johannesson, K.H., Tang, J., 2009. Conservative behavior of arsenic and other oxyanion-forming trace elements in an oxic groundwater flow system. J. Hydrol. 378, 13–28.
Kohler, C., et al., 2012. Extracytoplasmic function (ECF) sigma factor σ F is involved in Caulobacter crescentus response to heavy metal stress. BMC Microbiol. 12, 210.
Liu, Y.Y., et al., 2017. Coupled hydro-biogeochemical processes controlling Cr reductive immobilization in Columbia River hyporheic zone. Environ. Sci. Technol. 51, 1508–1517.
Meng, F.G., et al., 2009. Recent advances in membrane bioreactors (MBRs): membrane fouling and membrane material. Water Res. 43, 1489–1512.
Miao, Y., et al., 2017. Mechanisms of microbial community structure and biofouling shifts under multivalent cations stress in membrane bioreactors. J. Hazard. Mater. 327, 89–96.
Mutamim, N.S.A., et al., 2013. Membrane bioreactor: applications and limitations in treating high strength industrial wastewater. Chem. Eng. J. 225, 109–119.
Naz, I., et al., 2016. Effect of the chemical composition of filter media on the microbial community in wastewater biofilms at different temperatures. RSC Adv. 6, 104345–104353.
Nicholson, F.A., et al., 2003. An inventory of heavy metals inputs to agricultural soils in England and Wales. Sci. Total Environ. 311, 205–219.
Porter, S.S., et al., 2017. Association mapping reveals novel serpentine adaptation gene clusters in a population of symbiotic Mesorhizobium. ISME J. 11, 248–262.
Pradhan, S.K., et al., 2016. Bacterial chromate reduction: a review of important genomic, proteomic, and bioinformatic analysis. Crit. Rev. Environ. Sci. Technol. 1–45.
Samaras, P., et al., 2009. Effect of hexavalent chromium on the activated sludge process and on the sludge protozoan community. Bioresour. Technol. 100, 38–43.
Takada, K., et al., 2018. Cake layer bacterial communities during different biofouling stages in fullscale membrane bioreactors. Bioresour. Technol. 259, 259–267.
Thatoi, H., et al., 2014. Bacterial chromate reductase, a potential enzyme for bioremediation of hexavalent chromium: a review. J. Environ. Manag. 146, 383–399.
Trubitsyn, I.V., et al., 2014. Expansion of ability of denitrification within the filamentous colorless sulfur bacteria of the genus Thiothrix. FEMS Microbiol. Lett. 358, 72–80.
Vaiopoulou, E., Gikas, P., 2012. Effects of chromium on activated sludge and on the performance of wastewater treatment plants: a review. Water Res. 46, 549–570.
Vatsouria, A., et al., 2005. Anaerobic co-reduction of chromate and nitrate by bacterial cultures of Staphylococcus epidermidis L-02. J. Ind. Microbiol. Biotechnol. 32, 409–414.
Wang, C., et al., 2015. Dynamic fouling behavior and cake layer structure changes in nonwoven membrane bioreactor for bath wastewater treatment. Chem. Eng. J. 264, 462–469.
Xia, S.Q., et al., 2012. Effect of solids retention time on antibiotics removal performance and microbial communities in an A/O-MBR process. Bioresour. Technol. 106, 36–43.
Xia, S.Q., et al., 2010. The effect of organic loading on bacterial community composition of membrane biofilms in a submerged polyvinyl chloride membrane bioreactor. Bioresour. Technol. 101, 6601–6609.
Xia, S.Q., et al., 2015. Removal mechanism of low-concentration Cr (VI) in a submerged membrane bioreactor activated sludge system. Appl. Microbiol. Biotechnol. 99, 5351–5360.
Xiong, J.L., et al., 2016. Structural characteristics and development of the cake layer in a dynamic membrane bioreactor. Sep. Purif. Technol. 167, 88–96.
Yang, D.Z., et al., 2016. Model for seawater fouling and effects of temperature, flow velocity and surface free energy on seawater fouling. Chin. J. Chem. Eng. 24, 658–664.
Zhao, W., et al., 2009. Effect of hexavalent chromium on performance of membrane bioreactor in wastewater treatment. J. Environ. Eng.-ASCE 135, 796–805.
Zhong, L., et al., 2017. Nitrate effects on chromate reduction in a methane-based biofilm. Water Res. 115, 130–137.
Zhou, L., et al., 2014a. Effects of low-concentration Cr (VI) on the performance and the membrane fouling of a submerged membrane bioreactor in the treatment of municipal wastewater. Biofouling 30, 105–114.
Zhou, L., et al., 2014b. New insight into the effects of Ca (II) on cake layer structure in submerged membrane bioreactors. Biofouling 30, 571–578.
Zhou, L., et al., 2014c. Effects of suspended titanium dioxide nanoparticles on cake layer formation in submerged membrane bioreactor. Bioresour. Technol. 152, 101–106.
Zhu, Z.Y., et al., 2016. Cake properties as a function of time and location in microfiltration of activated sludge suspension from membrane bioreactors (MBRs). Chem. Eng. J. 302, 97–110.